Partitioning and Diffusion of Proteins and Linear Polymers in Polyacrylamide Gels

Jane Tong and John L. Anderson
Colloids-Polymers-Surfaces Program, Department of Chemical Engineering, Carnegie Mellon University, Pittsburgh, Pennsylvania 15213 USA

ABSTRACT The equilibrium partition coefficient (K) and diffusion coefficient (D^{gel}) of two proteins and two linear polymers were measured as a function of polymer content of a 2.7% cross-linked polyacrylamide (PA) gel. The gel concentration, expressed as a volume percentage of PA in the gel (ϕ), varied between 0 and 14%. The measurements were made by fluorescence spectroscopy; fluorescent dyes were covalently attached to the macromolecules. The dependence of K on ϕ for the proteins agrees with a model of the gel network as randomly placed, impenetrable rods. The diffusion data are interpreted in terms of an effective medium theory for the mobility of a sphere in a Brinkman fluid. Using values of the Brinkman parameter in the literature, the effective medium model with no adjustable parameters fits the diffusion data for the proteins very well but underpredicts D^{gel} for the linear polymers. The gel effect on partitioning is significantly greater than that on diffusion. The permeability (KD^{gel}) of bovine serum albumin decreased by 10^3 over the range $\phi = 0 \rightarrow 8\%$, and the ratio of permeabilities for ribonuclease compared to BSA increased from 2 to 30.

INTRODUCTION

Gels are attractive as separation devices because of their ability to essentially eliminate convective mixing and their selectivity for molecules based on size, charge, or chemical affinity. Gels are space-filling at low-volume fractions of the network material (e.g., cross-linked polymer). The high osmotic compressibility of charged hydrogels can be used to extract solutes on the basis of size and charge (Gehrke et al., 1986; Gehrke and Cussler, 1989; Vasheghani-Farahani et al., 1992). Recent commercial developments include rigid porous chromatographic particles with tailored gels fixed inside the pores to selectively remove proteins from solution (Boschetti, 1994; Boschetti et al., 1995). Gel matrices are also important components of tissue (Chary and Jain, 1989; Luby-Phelps et al., 1987) in that they control the traffic of macromolecular solutes between vascularized spaces. To design gels for particular biological separations or to properly model in vivo transport of solutes in tissue, the partitioning and diffusion of macromolecules in gels must be understood in terms of the physical properties of the gel and macromolecules.

The partition coefficient of a solute molecule (K) is defined as the equilibrium ratio of concentration in the gel (based on total gel volume) compared to the solution concentration:

$$K = \frac{C^{gel}}{C^{soln}}, \tag{1}$$

where C is expressed as solute mass per volume of the designated phase (solution or gel). In the absence of attractive interactions between the solute and gel network, K is less than 1 because the volume occupied by the network excludes the solute based on the solute's size. This excluded-volume effect depends on the volume fraction of the polymer forming the network (ϕ), the radius of the chains of the polymer, and the size and shape of the solute molecule. Ogston (1958) developed a model for the probability of placing rigid spheres of radius a in a matrix composed of long cylindrical fibers of radius a_f. His result can be expressed in the form

$$K = \exp\left[-\phi\left(1 + \frac{a}{a_f}\right)^2\right]. \tag{2}$$

Important assumptions in this model are 1) the solute/fiber interaction is purely hard-sphere in nature, 2) the fibers are infinitely long and were placed randomly in the matrix, and 3) the solute concentration is very low, so that solute-solute interactions are negligible in both phases. Fanti and Glandt (1990a,b) extended the theory to include effects of solute-solute interactions at higher concentrations in cases where $a > a_f$ and showed that K increases substantially when the volume fraction of the solute in solution exceeds about 2%.

Fawcett and Morris (1966) and Morris and Morris (1971) obtained values of K for globular proteins in cross-linked polyacrylamide-gel particles based on their data from size exclusion chromatography. They used the form of Eq. 2, which was originally proposed by Ogston (1958), to interpret their data. This form uses L = length of fiber per volume of gel instead of polymer volume fraction ϕ; this parameter is related to the volume fraction of the fibrous matrix and the fiber radius by $\phi = \pi a_f^2 L$. The Stokes-

Received for publication 18 September 1995 and in final form 5 December 1995.

Address reprint requests to Dr. John L. Anderson, Department of Chemical Engineering, Carnegie Mellon University, Pittsburgh, PA 15213. Tel.: 412-268-6986; Fax: 412-268-7139; E-mail: jlacheme@andrew.cmu.edu.

0006-3495/96/03/1505/09 $2.00

Einstein radius (a_s) of each protein was used for the effective radius a:

$$a_s = \frac{kT}{6\pi\eta D^{soln}}. \quad (3)$$

Fawcett and Morris let both L and a_f be adjustable parameters for a given gel; however, they did not report values of ϕ from which one could check the best-fit value of L. At a given cross-link density (CL), L was proportional to the total mass of polymer used per volume of reaction, which is expected. An unexpected result was that L depended on CL at a given mass of polymer and showed a maximum value at 3% cross-link. The best-fit values of a_f were relatively independent of the total mass of polymer in the gel as expected, but a_f increased from 5.3 to 10.2 Å for an increase of CL from 1% to 5%. The variation in a_f might have been due to bundling of polyacrylamide (PA) chains or heterogeneities in the gel microstructure caused by the cross-linking.

The hydrodynamic effects of fixed obstacles on the mobility of hard spheres has been calculated for well-defined geometric arrangements of the obstacles (e.g., Howells, 1974; Phillips et al., 1989, 1990). Effective-medium models for gels and other porous media represent the hydrodynamic effects of the obstacles by one material parameter of the fluid, for example, the Darcy permeability (κ^{-2}), which appears in the Brinkman model. The excess hydrodynamic drag due to the network depends on two parameters: the hydrodynamic screening length κ^{-1} and the size of the diffusing molecule (a = radius). The friction coefficient of a sphere translating through a Brinkman fluid at low Reynolds was first derived by Brinkman (1947). Using the Einstein equation, which relates the diffusion and friction coefficients, Brinkman's result gives

$$\frac{D^{gel}}{D^{soln}} = \frac{1}{1 + \kappa a + \frac{1}{3}(\kappa a)^2}. \quad (4)$$

Taking a_s (see Eq. 3) for the radius of the solute, the Brinkman model has only one parameter, κ, which is presumably only a function of the gel's microstructure. This hydrodynamic parameter can be estimated from a geometric model for the network (e.g., see Phillips et al., 1989) or calculated from the Darcy permeability, which is a measurable property of the gel. Note that the Brinkman model does not account for several factors of potential importance: Brownian motion of the gel network itself (Sellen, 1987; Park et al., 1990), near-field hydrodynamic effects of the polymer network on the diffusing solute (i.e., a breakdown of the effective medium approximation on a length scale of a_f), and the obstacle effect of the polymer network, which requires the solute to diffuse around the polymer chains. Nevertheless, Eq. 4 has had some success in correlating data for the diffusion of proteins in entangled polymer solutions (Phillips et al., 1989; Laurent and Pietruszkiewicz, 1961; Laurent et al., 1963).

Johnson et al. (1995a) proposed a modified Brinkman model to include the obstacle (tortuosity) effect of the gel on the diffusing solute:

$$\frac{D^{gel}}{D^{soln}} = \frac{\exp(-0.84\Phi^{1.09})}{1 + \kappa a + \frac{1}{3}(\kappa a)^2}, \quad (5)$$

where

$$\Phi = \phi\left(1 + \frac{a_s}{a_f}\right)^2.$$

The numerator is an empirical fit of the Brownian dynamics simulations performed by Johansson and Löfroth (1993) for values of $\Phi < 3$. The numerator of Eq. 5 accounts for the tortuous path facing a solute molecule diffusing through the network of obstacles forming the gel.

In this paper we report experimental results for the partition and diffusion coefficients of two globular proteins and a linear polymer of two molecular weights in PA gels. The cross-link density was fixed at 2.7%. PA gels are neutral and generally do not bind to macromolecules that are soluble in water. They are thought to be networks of single polymer chains held together by chemical cross-links. There is an extensive literature on the chemical synthesis (Fawcett and Morris, 1966; Chrambach and Rodbard, 1972), physical properties (Janas et al., 1980; Tanaka, 1981; Hsu and Cohen, 1984; Hecht et al., 1985; Sellen, 1987; Baselga et al., 1987; Geissler et al., 1988), and phase transitions (Dusek, 1993) of PA gels. Light scattering measurements (Patterson, 1987; Sellen, 1987; Park et al., 1990) indicate that the polymer network has a significant Brownian motion.

We have measured both the partition coefficient and diffusion coefficient of proteins and synthetic polymers as a function of gel volume fraction; the measurement of both these parameters on the same gel represents the uniqueness of this work. The following questions are addressed. First, does Eq. 2 describe the partitioning of approximately spherical proteins up to volume fractions as high as 14%? Second, does Eq. 2 apply to linear polymers whose size and shape can only be described statistically? If so, what is the appropriate size a of linear polymers? Third, how well does Eq. 4 or 5 describe the diffusion of proteins and linear polymers in gels? Finally, how does the macrosolute permeability (KD^{gel}) vary with solute size and gel volume fraction?

EXPERIMENTS

Complete details of the experimental procedures are given by Tong (1995). A summary is presented below.

Gels

The gels were made by copolymerizing acrylamide and *N,N'*-methylene-bisacrylamide in deionized and filtered water. The cross-link density, which is defined as the ratio of

the mass of cross-linker (bisacrylamide) to the mass of monomer (acrylamide), was 2.7% for all the experiments. The initiator was ammonium persulfate and the promoter was tetramethyl ethylene diamine. The polymerization reaction proceeds by a free-radical mechanism at room temperature (~25°C). The reaction reaches 90% completion of the monomer and cross-linker within 60 min and is essentially complete after 3 h (Righetti et al., 1981; Tobita and Hamielec, 1990). An important step in the procedure is to rid the system of oxygen. All reactants were purchased from BioRad Laboratories (electrophoresis grade; Hercules, CA).

After mixing the reactants, the mixture was placed between two glass plates spaced 0.76 mm apart. The polymerization occurred for more than 3 h at room temperature and the resulting gel "slab," confined between the glass plates, was stored in a sealed bag with 0.02% (by weight) sodium azide aqueous solution at 7°C. To perform an experiment, a square piece of the gel was cut from the slab and soaked in a borate buffer (pH ~10) for 1 h before being placed in the solution of dye-labeled macromolecules at room temperature for a time τ_{eq} sufficient to reach equilibrium. τ_{eq} was calculated from the solution to Fick's second law for diffusion into a planar film using estimated values of the partition and diffusion coefficients. Tests were done to ensure that τ_{eq} was sufficient to achieve equilibrium partitioning. The equilibrated gel was then placed between two Pyrex disks spaced by a Viton gasket 0.76 mm thick. The piece of gel occupied only part of the volume defined by the gasket; solution in equilibrium with the gel occupied the remainder of the space, thus providing us a way to achieve an in situ calibration of the fluorescence from the dye-labeled macromolecules in solution. The disks were clamped together to contain the gel when it was mounted into a lens holder and placed in the optical train for the fluorescence experiments.

The volume fraction of polyacrylamide plus cross-linker in the gel was determined by first weighing a piece of the hydrated gel and then evaporating the water and weighing the residue. Letting m_w, m_b, and m_p be the mass of the water, buffer, and polymer (PA), respectively, then

$$\phi = \frac{m_p v_p}{m_p v_p + (m_w + m_b) v_{wb}}. \quad (6)$$

The partial specific volume (v_p) of PA in water is 0.70 cm^3/g (Munk et al., 1980), and v_{wb} is 1.01 cm^3/g, as determined experimentally. The masses m_w and $m_p + m_b$ were determined by weighing the hydrated and dehydrated gel, and m_b/m_w was known from the make-up of the electrolyte solution.

A buffer (0.0125 M sodium borate, 0.018 M NaOH) was used to control the pH at ≈10. Fluorescence increases with pH but levels off at about pH 9. The emission of fluorescence was determined to be nearly the same at pH 9.2 and pH 10.

TABLE 1 Diffusion coefficients taken from literature and measured by FRAP experiments (in pH 10 sodium borate buffer and I = 0.043 M), corrected to 20°C

Solute	MW	a_s (Å)	$D_{literature}$ (10^{-7} cm^2/s)	D_{expt} (10^{-7} cm^2/s)	Polydispersity Index*
RNase	13,700	20	10.7¶	11.1 ± 0.5§	1
BSA	67,000	36	5.9‡	6.0 ± 0.5	1
PEG 5K	5,160	20	10.9‖	10.0 ± 0.9	1.04
PEG 12.6K	12,320	31	6.9‖	6.5 ± 0.6	1.05

The Stokes-Einstein radius (a_s) was calculated from the $D_{literature}$ and Eq. 4.
*Proteins are taken to be monodisperse (confirmed by differential scanning calorimetry), and the polydispersity of PEGs is given by the supplier.
‡Average value of Wagner and Scheraga (1956) and Anderson et al. (1978).
§The standard deviation of D_{exp} is determined by the propagation of errors method (Tong, 1995).
¶Creeth (1958).
‖Interpolated values from Rempp (1957) and Elias (1961).

Macromolecules

Four macromolecules were studied: two globular proteins, bovine serum albumin (BSA) and ribonuclease-A (RNase); and two different molecular weights of a linear polymer, poly(ethylene glycol) (PEG). The properties of these solutes are summarized in Table 1. The RNase (R-5000; Sigma Chemical Co., St. Louis, MO) was dialyzed against a phosphate buffer (pH 6.5) for 2 h to remove impurities and then heated to 60°C for 10 min to dissociate aggregates (Tilton, 1991). The sample was then dialyzed for 2 h against a 0.1 M sodium borate buffer (pH 9.2). The BSA (A-7511; Sigma Chemical Co.) was used as received and dissolved in the same borate buffer.

The proteins were labeled with the fluorescent dye fluorescein-5-isothiocyanate (FITC, Isomer I; Molecular Probes, Eugene, OR) (Lok et al., 1983). The molar ratio of dye to protein was about 1 for both proteins. The dye-labeled protein was separated from free (unreacted) dye by size exclusion chromatography (BioGel P-6; BioRad Laboratories, Hercules, CA). The final labeling ratios (average number of FITC molecules bound per protein molecule) were typically 0.80–0.95 for BSA and 0.60–0.80 for RNase.

The PEG polymer standards were used as received. The 5000 MW fraction was obtained from Pressure Chemical Co. (Pittsburgh, PA) and the 12,600 MW fraction was obtained from Polymer Laboratories (Amherst, MA). The polymers were labeled with 5-([4,6-dichlorotriazin-2-yl]amino)-fluorescein (DTAF, D-0531; Sigma Chemical Co.). The unreacted DTAF was separated from the labeled polymer by chloroform extraction and ion-exchange chromatography (Johansson et al., 1983). The final labeling ratio was less than 1.

Measurement of partition coefficient

The partition coefficient (see Eq. 1) was determined by measuring the concentration of the dye-labeled macromolecule in solution (C^{soln}) and in the gel (C^{gel}) after equili-

bration. Concentrations were determined from the measured fluorescence intensities and appropriate calibrations.

Fig. 1 shows the configuration of the gel in the sample holder (between the glass disks). The fluorescence intensity is denoted by F, with the subscript indicating the path of the laser beam as depicted in the figure. F_g is the fluorescence signal from labeled protein within the gel, and F_s is the fluorescence from the solution over the same path length as the gel thickness.

Because the concentration of labeled protein is proportional to the fluorescence signal (Tong, 1995), the partition coefficient is given by

$$K = \frac{F_g}{F_s} = \frac{F_{g+sl} - F_{sl}}{F_{s+sl} - F_{sl}}. \quad (7)$$

The signal F_{sl} was not directly measurable but instead was determined from the other measurements as follows:

$$F_{sl} = \frac{F_{g+sl} - F_{g+bl}}{1 - F_{b+bl}/F_{s+sl}}. \quad (8)$$

K was determined by combining Eqs. 7 and 8; therefore, four measurements were needed: F_{g+sl}, F_{s+sl}, F_{g+bl}, and F_{b+bl}. The latter two were made by removing the gel slab from the sample holder, rinsing the surfaces of the gel and disks with buffer solution, placing the slab back into the sample holder and filling the void space with buffer, and then measuring the fluorescence signals. The time required to dismantle the holder, rinse the gel slab with buffer, and replace the gel in the holder to take the measurements of F_{g+bl} and F_{b+bl} was orders of magnitude smaller than the equilibration time for macromolecule transport between the gel and solution.

There are two potential sources of error due to "probe effects." First, the fluorescence emission spectrum of the dye might be affected by the PA gel; and second, the dye attached to the macromolecule might adsorb or bind to the polymer network of the gel and thus bias K. We experimentally tested for both of these potential effects and found them to be absent (Tong, 1995).

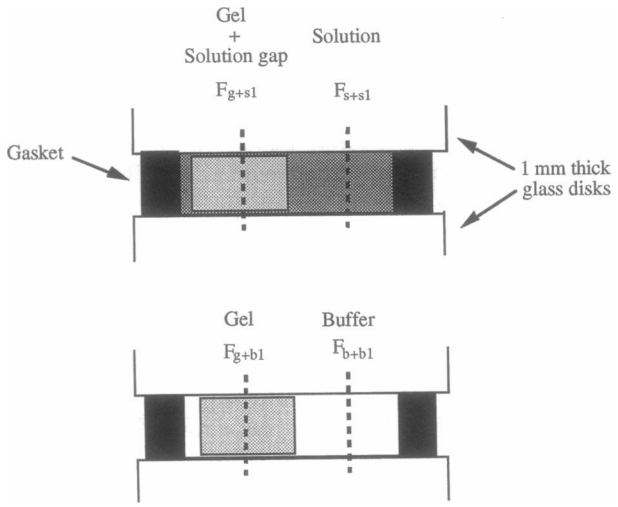

FIGURE 1 Determination of K by measuring four different fluorescence intensities, F, in the gel sample holder. Subscript g denotes the fluorescence signal from the labeled protein within the gel, and subscript s is the fluorescence from the labeled-protein (or PEG) solution in the absence of the gel over the same thickness as the gel. Subscript sl is the fluorescence of the solution in the thin gap between the gel and the surface of the glass disk. Subscripts b and bl have similar meanings, except that there is no labeled protein in the buffer solution.

Diffusion experiments

After measuring the fluorescence values F_{g+bl} and F_{b+bl}, the diffusion coefficient of the macromolecule within the gel was measured using fluorescence recovery after photobleaching (FRAP). We used the technique known as "spot" FRAP (Axelrod et al., 1976; Simon et al., 1988). A laser beam (λ = 488 nm) was focused as a circular region of characteristic radius w onto the gel. An optical cut-off filter (λ = 515 nm) was used to select the appropriate wavelength for the maximum fluorescence emission (520 nm) from the dye. Because the gel was thin (<1 mm) and transparent, the spot radius was constant throughout the thickness of the gel. The experiment was started by amplifying the intensity of the incident beam by several orders of magnitude for a short time (typically 0.1 s) and then cutting back the power to the normal monitoring level. The short pulse of high-intensity radiation "bleached" some of the fluorescent dye molecules (typically 20–30%) so they became inactive with respect to a fluorescent signal. Because these dye molecules were bound to mobile macromolecules that continually diffuse within the gel, the fluorescence signal from the illuminated spot recovered with time. By tracking this recovery and modeling it as a diffusion process, we determined the self-diffusion coefficient D for the macromolecule.

The modeling of FRAP has two parts (Axelrod et al., 1976). First, the photobleaching step is assumed to be a first-order reaction (with respect to the labeled solute concentration). Account must be taken of the gaussian nature of the intensity (I) of the beam:

$$I(r) = \frac{2P_o}{\pi w^2}\exp\left(-\frac{2r^2}{w^2}\right), \quad (9)$$

where r is the radial distance from the center of the beam, P_o is the total power of the laser beam, and w is the beam radius. The second part is to model the recovery by Fick's second law of diffusion:

$$\frac{\partial C}{\partial t} = D\frac{1}{r}\frac{\partial}{\partial r}\left(r\frac{\partial C}{\partial r}\right), \quad (10)$$

where C is the concentration of the labeled macromolecule within the sample and D is the diffusion coefficient of the macromolecule. The measured fluorescence emission F is

given by

$$F(t) = \frac{q}{A}\int_0^\infty C(r,t)I(r)2\pi r dr. \quad (11)$$

q is the product of the quantum efficiencies of light absorption, emission, and detection; A is the attenuation factor of the laser beam. Neither q nor A is required to determine D, because the fluorescence signals are always normalized by the initial value F_i before photobleaching. The following expression is obtained by solving Eq. 10 and substituting the result and Eq. 9 into Eq. 11 (Axelrod et al., 1976):

$$F(t) = F_i\sum_{n=0}^{\infty}\frac{(-K_b)^n}{n!}\frac{1}{1+n(1+2t/t_D)} \quad (12)$$

$$F(0^+) = F_i\frac{(1-\exp(-K_b))}{K_b},$$

where F_i is the measured value of F before the photobleaching step and $F(0^+)$ is the fluorescence signal immediately after the photobleaching step. The diffusion time is related to the beam radius and diffusion coefficient by

$$t_D = \frac{w^2}{4D}. \quad (13)$$

The two unknown parameters, t_D and K_b, can be determined by fitting Eq. 12 to the data F versus t. This approach assumes total recovery of the fluorescence signal after long times ($F \to F_i$ as $t \to \infty$).

Over the time scale of the experiment (on the order of minutes), it was often not possible to get a good fit of the data to Eq. 12 because not all of the macromolecules appeared to be mobile. To improve the fit, we assumed that only a fraction f_m of the labeled macromolecules were "mobile" and the fraction $(1 - f_m)$ did not diffuse. The mobile and immobile fractions were assumed to have equal probability of being bleached. The mobile fraction is related to the measured fluorescence before and immediately after photobleaching and at "infinite" time ($t \gg t_D$) after recovery by the following expression:

$$f_m = \frac{F(\infty) - F(0^+)}{F_i - F(0^+)}. \quad (14)$$

Equation 12 is replaced by the following:

$$\frac{F(t)}{F_i} = f_m\left[\sum_{n=0}^{\infty}\frac{(-K_b)^n}{n!}\frac{1}{1+n(1+2t/t_D)}\right] + (1-f_m)\frac{F(0^+)}{F_i}, \quad (15)$$

where K_b is defined in Eq. 12. The first term represents the fluorescence of the mobile species, which is time dependent, and the second term represents the fluorescence of the immobile species, which is constant. Now three parameters are used to fit the data for F versus t: t_D, K_b, and f_m. The diffusion coefficient for the macromolecule is obtained from the best-fit value of t_D and Eq. 13. Simulations using parameter values appropriate for our experiments indicate that truncating the series of Eq. 15 after $n = 8$ describes the curve $F(t)$ to within 1% of the characteristic time t_D for a Monte Carlo simulation with 2% random fluctuations in the simulated data (Tong, 1995).

Equation 13 implies that it is important to know the beam radius w. The value of w was determined by a beam-blocking technique (Khosrofian and Garetz, 1983); using this technique we verified that the laser beam was gaussian (Tong, 1995). Note, however, that the results are relatively insensitive to w because we are primarily concerned with the ratio D^{gel}/D^{soln}, and both determinations were done with the same beam; thus, $D^{gel}/D^{soln} = t_D^{soln}/t_D^{gel}$. Experiments performed with different values of w for D^{gel} and D^{soln} showed t_D to be proportional to w^2, as predicted by the model. Furthermore, the relatively good agreement between our measurements of D^{soln} and the literature values (see Table 1) indicates that we knew the value of w to within acceptable accuracy.

RESULTS AND DISCUSSION

Partitioning coefficient

Fig. 2 shows the results for the proteins. The broken curves are best fits of Eq. 2, using a_s for the protein radius; the best-fit values of a_f are 7.2 Å for RNase and 5.9 Å for BSA. In determining the value of a_f, we only used the open symbols in the least-squares (χ^2 minimization) analysis because these results are averages of data from at least two cuts of the same gel slab. The filled symbols represent data

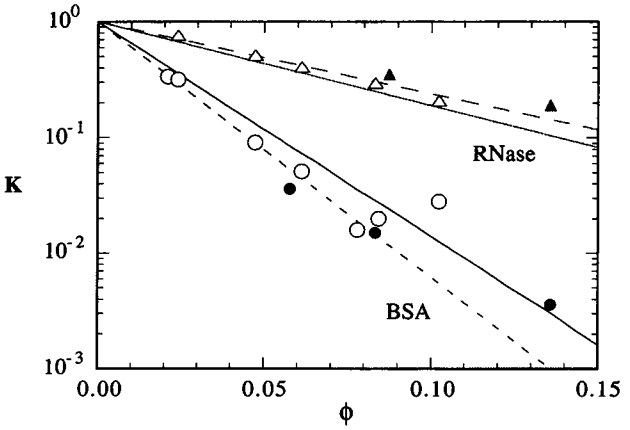

FIGURE 2 Partition coefficient (K) of RNase (△, ▲) and BSA (○, ●) versus gel volume fraction (ϕ). The open symbols are average values from at least two different cuts of the same gel slab, and the filled symbols represent a single piece of the gel slab. The data were fitted to Eq. 2 (– – –) using only the open symbols by adjusting the fiber radius a_f (7.2 Å for RNase, 5.9 Å for BSA) and using a_s (see Eq. 3) for the protein radius. The solid lines are Eq. 2, with a_f = 6.5 Å. The size of the symbols approximately equals the standard deviation of the data from different pieces of one gel.

for only one piece of the gel and were not used in fitting Eq. 2 to the data. The solid lines in Fig. 2 were computed assuming a_f = 6.5 Å for both proteins. It is our opinion that Eq. 2 with this value of a_f gives a reasonable representation of the data. Our value of a_f, 6.5 Å, is comparable to that obtained by others based on fitting Eq. 2 to partitioning data for various compact proteins (Fawcett and Morris, 1966; Morris and Morris, 1971; Sellen, 1987).

The results for the linear polymers are plotted in Fig. 3. The lines drawn through the data are best fits to Eq. 3, assuming a_f = 6.5 Å. The best-fit values of a are

$$a = 23 \text{ Å} \quad \text{for} \quad \text{PEG 5K}$$

$$a = 37 \text{ Å} \quad \text{for} \quad \text{PEG 12.6K}. \tag{16}$$

Because these macromolecules are linear polymers, it is not clear what the proper size is for partitioning. The ratio of exclusion radius (a) to Stokes-Einstein radius (a_s; see Table 1) is 1.2 for both polymers. Theories based on mean projected half-length of the molecule (Casassa, 1976) suggest that for a random-flight linear polymer chain near a flat wall, the equivalent partitioning radius is $(2/\sqrt{\pi})r_g$, where r_g is the radius of gyration of the polymer, which generally is larger than a_s. A model for the exclusion of linear polymer chains near cylindrical fibers is not available.

Diffusion coefficient

Figs. 4 and 5 are plots of the normalized diffusion coefficients versus PA volume fraction. Immediately noticeable is the small variation of D^{gel} with ϕ compared to variations in the partition coefficient. This means that the selectivity of a gel based on macromolecule size is determined primarily by the equilibrium partitioning between the solution and gel phases rather than by diffusion.

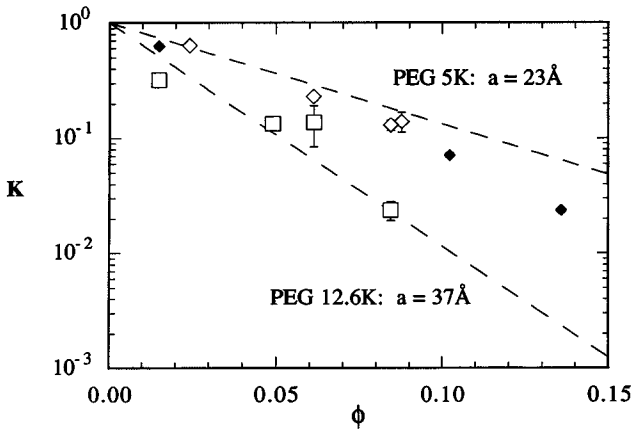

FIGURE 3 Partition coefficient of PEG versus gel volume fraction. The open and filled symbols have the same meaning as in Fig. 2. The broken lines represent the best fit (see Eq. 16) of the polymer molecular radius (a) for a fiber radius a_f = 6.5 Å in Eq. 3.

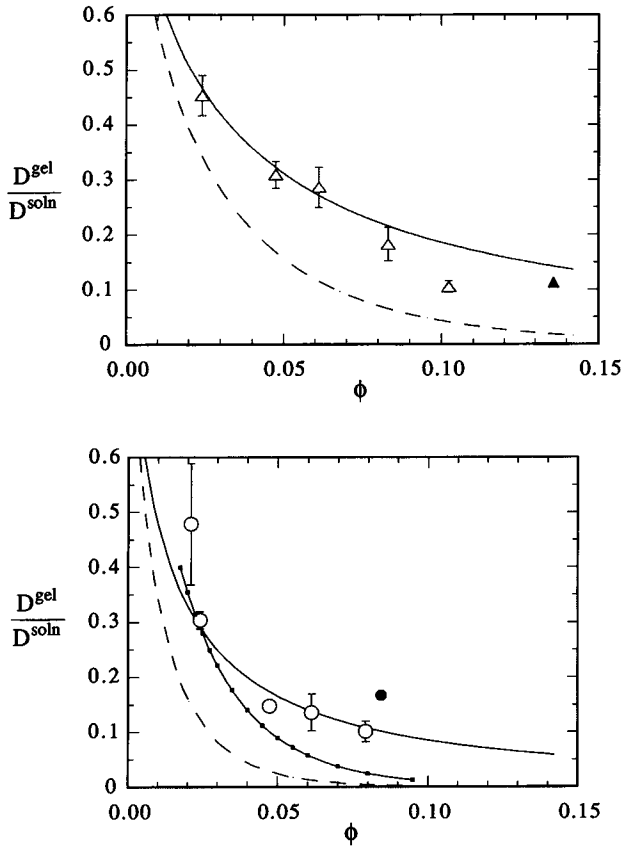

FIGURE 4 (a) Hindered diffusion of RNase versus the volume fraction of polyacrylamide gel. The open and filled symbols have the same meaning as in Fig. 2. The solid curve represents Brinkman's model (Eqs. 4 and 18). The broken curve includes the steric hindrance of the fibers (Eq. 5). (b) Hindered diffusion of BSA versus the volume fraction of polyacrylamide gel. The open and filled symbols have the same meaning as in Fig. 2. The solid curve with squares is the experimental data of Park et al. (1990) for BSA at 5% cross-link, as given by Eq. 17 of this paper.

Our data for BSA are compared with the results of Park et al. (1990) in Fig. 4 b. Their results were obtained by holography relaxation spectroscopy over length scales of order 3 μm, about 40 times smaller than our length scales ($w \approx 120$ μm). Their data are correlated by the following expression:

$$\frac{D^{gel}}{D^{soln}} = \exp(-27.3\rho^{0.92}) = \exp(-37.9\phi^{0.92}), \tag{17}$$

where we have assumed $\phi = v_p\rho$ and v_p = 0.7 cm^3/g. Park et al. did not measure the final polymer concentration of the gel; hence their reported concentrations of PA in the network could be in error because of swelling or deswelling of the gel after polymerization. This could explain some of the discrepancy between our data and theirs. The discrepancies could also be due to differences in cross-link density (5.3% for Park et al., 2.7% for us) and to the different length scale of their measurement.

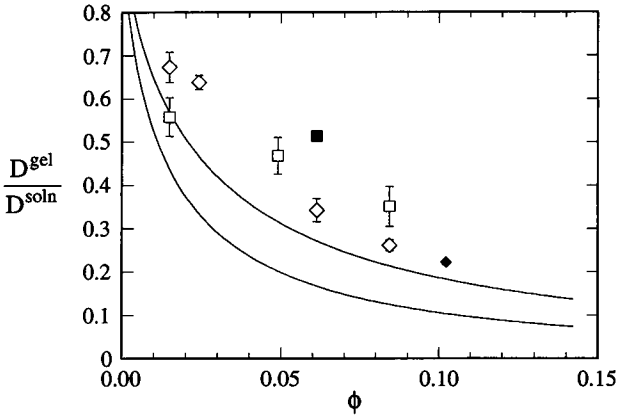

FIGURE 5 Hindered diffusion of PEG 5K (◇, ◆) and PEG 12.6K (□, ■) versus gel volume fraction. The open and filled symbols have the same meaning as in Fig. 2. The solid curves represent Eqs. 4 and 18 for a_s = 20 and 31 Å.

To test the Brinkman-based models (Eqs. 4 and 5) against our diffusion data, we require the hydrodynamic parameter κ as a function of gel volume fraction. Tokita (1993) measured the Darcy permeability (κ^{-2}) of 2.2% cross-linked PA gels. Transcribing the permeability data from the figures in his paper, we obtained the following empirical correlation:

$$\kappa^{-2} = 2.64 \times 10^{-16}\phi_i^{-1.42}, \qquad (18)$$

where ϕ_i is the volume fraction determined from the initial monomer plus cross-linker concentration (g/ml) before polymerization. Tokita (1993) claimed that the gel volume was kept constant in the apparatus during the permeability (pressure drop-flowrate) measurements, so that the gel was prevented from swelling ($\phi = \phi_i$). By comparing Eq. 18 with the semi-empirical relation derived by Jackson and James (1986),

$$(\kappa a_f)^2 = -\frac{20}{3}\frac{\phi}{(\ln\phi + 0.931)}, \qquad (19)$$

we find a_f = 5.5 Å, which is comparable to the value (6.5 Å) obtained from the partitioning data.

The Brinkman-based models, using Eq. 18 for κ, are compared with the diffusion data for the two proteins in Fig. 4, *a* and *b*. Eq. 4 (*solid lines*) shows good agreement with the data, without the use of any adjustable parameters. The broken lines in the figures are calculations from Eq. 5 with a_f = 6.5 Å. This equation has a correction for the obstacle effect, that is, the solutes must diffuse around the polymer fibers. Clearly, inclusion of the steric correction (*broken curve*) destroys the agreement between theory and experiment. One explanation is that the Brownian motion of the polymer chains of the gel network couples with the solute diffusion, thereby mitigating the steric effect, which was derived based on a static configuration of network fibers (Johansson and Löfroth, 1993).

The Brinkman model, Eq. 4, is compared with the diffusion data for the linear polymers in Fig. 5. The agreement is not particularly good; the theory underpredicts the diffusion coefficient in the gel. There is only a weak effect of molecular weight on the hindered diffusion ratio of the PEGs. Haggerty et al. (1988) likewise reported an insensitivity of the hindered diffusion ratio to the molecular weight of linear polymers.

Solute permeability versus PA volume fraction

The solute permeability of a gel is proportional to the product of K times D^{gel}. A plot of this product against gel volume fraction is made in Fig. 6. The solid lines are theoretical predictions for the two proteins based on Eqs. 2–4 and 18 with a_f = 6.5 Å:

$$KD^{gel} = \frac{\exp[-\phi(1 + a_s/a_f)^2]}{1 + \kappa a_s + 1/3(\kappa a_s)^2} D^{soln}. \qquad (20)$$

Two important observations are noted. First, the gel volume fraction has a strong effect on the solute permeability; the variation is three orders of magnitude for BSA. Most of the selectivity (two orders of magnitude) is due to the variation in K. Second, there is a significant effect of macrosolute size. For example, a PA gel of volume fraction 8% is 30 times more permeable to RNase than to BSA, even though the ratio of molecular radii (and hence D^{soln}) is only 1.8. This type of selectivity is has not been demonstrated with open-pore membranes (Kim and Anderson, 1991). Fig. 6 is a clear illustration of the improved molecular selectivity that is possible with gels.

Fractional recovery in the diffusion experiments

Over the time scales of our FRAP experiments (on the order of 100-4000 s), there appeared to be incomplete recoveries of the fluorescence intensity from the bleached spot in some of the gels. The factor f_m was introduced (see Eq. 15) to

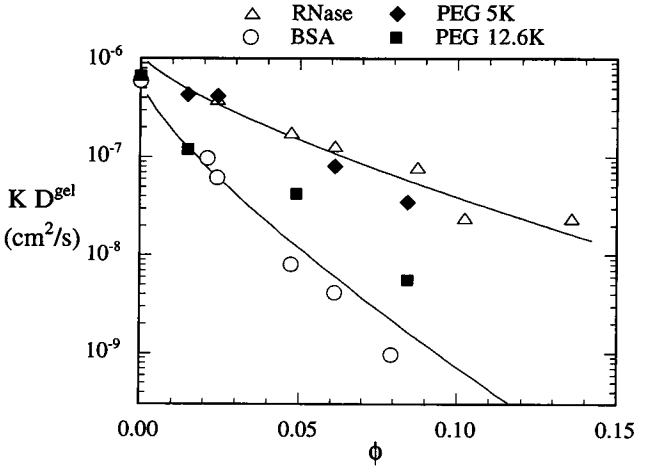

FIGURE 6 The diffusive permeability (KD^{gel}) versus gel volume fraction. The solid lines represent the Ogston-Brinkman model, Eq. 20, with a_f = 6.5 Å, applied to the protein data only.

allow for partial recovery. The question is: What is the physical meaning of partial recovery? Is it due to binding of dye-labeled macrosolutes to the gel? Or is it the result of a breakdown of Fick's law of diffusion on short time scales due to inhomogeneities in the gel (Nagle, 1992)?

The experimental values of f_m are plotted in Fig. 7. To see if incomplete recovery was due to irreversible binding of the dye-labeled solutes to the gel, we immersed pieces of gel that had been equilibrated with FITC-BSA in a BSA-free solution and measured how much protein was extracted after several days. In all cases, including the gels for which f_m was the smallest, there was complete recovery of the protein. This means that the fractional recoveries were not due to irreversible binding of the protein to the PA. An indication that fractional recoveries are the result of heterogeneities in the gel, resulting in partial trapping of proteins over short time scales, is that f_m is lower for BSA than for RNase; this is expected because BSA is significantly larger than RNase. This hypothesis is further supported by the trend of f_m decreasing with increasing ϕ. A more quantitative study of f_m versus macrosolute size might provide insight into the microscopic heterogeneities of polymeric gels.

Another indication that these gels are nonuniform on a local scale (~100 μm) is the fact that the standard deviation of K and D^{gel}/D^{soln} for measurements on different areas of the same piece of a gel of higher volume fractions was typically 10% of the mean. This standard deviation is well outside the error estimates made from instrumentation alone (Tong, 1995). There were comparable variations between different pieces of the same gel. It is not even certain that two gels made in an identical fashion would produce exactly the same properties, for example, gel volume fraction ϕ. The reactivity of the cross-linking agent vis-à-vis the monomer chain addition could also play a large role in determining the final structure of the gel.

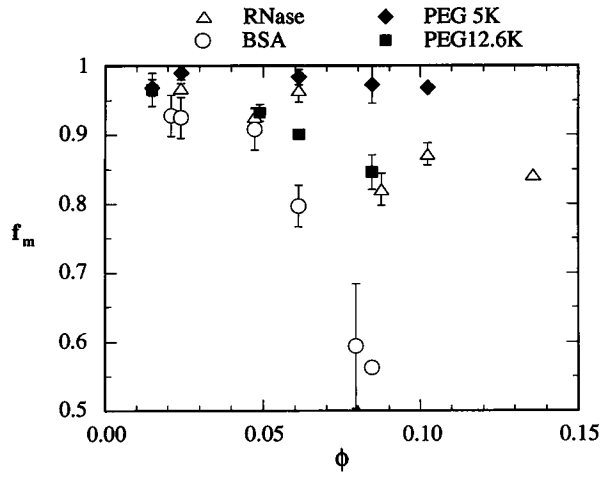

FIGURE 7 Fractional recovery versus gel volume fraction for the diffusion experiments.

SUMMARY

Ogston's excluded volume model (Eq. 2) fits the partitioning data over the range in gel volume fraction of $0 \rightarrow 0.14$ for globular proteins and linear polymers in neutral PA gels. Our estimate of equivalent chain radius, $a_f = 6.5$ Å, is in reasonable agreement with other researchers. The Stokes-Einstein radius (a_s) is taken for the size of the two proteins, whereas $a = 1.2\ a_s$ for the two linear polymers. The effect of the gel on the diffusion coefficient is semiquantitatively described by the hydrodynamic theory based on treating the gel as a Brinkman fluid. Equations 4 and 18 with no adjustable parameters are in good agreement with the protein data; however, the model underpredicts the diffusion data of the linear polymers. An unexplained result is that D^{gel}/D^{soln} is about the same for two samples of PEG, although their molecular weights differ by a factor of 2.5.

The solute permeability (KD^{gel}) of 2.7% cross-linked PA gels depends strongly on the gel volume fraction and macrosolute size. Fig. 6 demonstrates that enhanced selectivity based on molecular size is possible with neutral gels such as polyacrylamide. The enhanced selectivity is due primarily to the partitioning effect of the gel based on excluded volume. Biological transport processes and separations that depend on both the macromolecule partitioning into a gel and diffusing through the gel should demonstrate this selectivity.

The fact that not all of the fluorescence signal was recovered over the time scale of our diffusion experiments (τ_{expt}), even though there was total recovery of the protein from the gels over times of order $100\tau_{expt}$, implies that the diffusive processes were not completely Fickian, a possibility raised by Nagle (1992). Heterogeneities in local gel volume fraction over length scales of order $(D^{gel}\tau_{expt})^{1/2} \approx$ 150 μm could explain both observations. Such heterogeneities could trap some macrosolutes in regions of this size for times of order τ_{expt}, but the escape of macrosolutes from these traps by Brownian motion would be possible over time scales that are orders of magnitude greater than τ_{expt}. Because the length scale of diffusion (w) and thus the time of recovery can be varied with FRAP, it might be possible to probe microscopic heterogeneities in the gel structure with this technique.

We are very grateful for the technical advice and ideas given to us by Fred Lanni and Bob Tilton.

This research was supported by the Petroleum Research Fund of the American Chemical Society (grant 25294-AC7E) and the National Science Foundation (grant CTS-9122573). JT was also supported by a fellowship from the W. M. Keck Foundation (grant 880995).

REFERENCES

Anderson, J. L., F. Rauh, and A. Morales. 1978. Particle diffusion as a function of concentration and ionic strength. *J. Phys. Chem.* 82: 608–616.

Axelrod, D., D. E. Koppel, J. Schlessinger, E. Elson, and W. W. Webb. 1976. Mobility measurement by analysis of fluorescence photobleaching recovery kinetics. *Biophys. J.* 16:1055–1069.

Baselga, J., I. Hernandez-Fuentes, I. F. Pierola, and M. A. Llorente. 1987. Elastic properties of highly cross-linked polyacrylamide gels. *Macromolecules.* 20:3060–3065.

Boschetti, E. 1994. Advanced sorbents for preparative protein separation purposes. *J. Chromatogr. A.* 658:207–236.

Boschetti, E., L. Gurrier, P. Girot, and J. Horvath. 1995. Preparative high-performance liquid chromatographic separation of proteins with hyperD ion-exchange supports. *J. Chromatogr. B.* 664:225–231.

Brinkman, H. C. 1947. A calculation of the viscous force exerted by a flowing fluid on a dense swarm of particles. *Appl. Sci. Res.* A1:27–34.

Casassa, E. F. 1976. Comments on exclusion of polymer chains from small pores and its relation to gel permeation chromatography. *Macromolecules.* 9:182–185.

Chary, S. R., and R. K. Jain. 1989. Direct measurement of interstitial convection and diffusion of albumin in normal and neoplastic tissues by fluorescence photobleaching. *Proc. Natl. Acad. Sci. USA.* 86: 5385–5389.

Chrambach, A., and D. Rodbard. 1972. Polymerization of polyacrylamide gels: efficiency and reproducibility as a function of catalyst concentrations. *Separation Sci.* 7:663–703.

Creeth, J. M. 1958. Studies of free diffusion in liquids with the Rayleigh method. III. The analysis of known mixtures and some preliminary investigations with proteins. *J. Phys. Chem.* 62:66–74.

Dusek, K., editor. 1993. Responsive Gels: Volume Transitions I and II, Advances in Polymer Science. Springer-Verlag, New York.

Elias, H. G. 1961. Osmose an permeablen membranen. *Z. Phys. Chem.* 28:303–321.

Fanti, L. A., and E. D. Glandt. 1990a. Partitioning of spherical particles into fibrous matrices. 1. Density-functional theory. *J. Colloid Interface Sci.* 135:385–395.

Fanti, L. A., and E. D. Glandt. 1990b. Partitioning of spherical particles into fibrous matrices. 2. Monte Carlo simulation. *J. Colloid Interface Sci.* 135:396–404.

Fawcett, J. S., and C. J. O. R. Morris. 1966. Molecular-sieve chromatography of proteins on granulated polyacrylamide gels. *Separation Sci.* 1:9–26.

Gehrke, S. H., G. P. Andrews, and E. L. Cussler. 1986. Chemical aspects of gel extraction. *Chem. Eng. Sci.* 41:2153–2160.

Gehrke, S. H., and E. L. Cussler. 1989. Mass transfer in pH-sensitive hydrogels. *Chem. Eng. Sci.* 44:559–566.

Geissler, E., A. Hecht, F. Horkay, and M. Zrinyl. 1988. Compressional modulus of swollen polyacrylamide networks. *Macromolecules.* 21: 2594–2599.

Haggerty, L., J. H. Sugarman, and R. K. Prud'homme. 1988. Diffusion of polymers through polyacrylamide gels. *Polymer.* 29:1058–1063.

Hecht, A., R. Duplessix, and E. Geissler. 1985. Structural inhomogeneities in the range 2.5–2500 Å in polyacrylamide gels. *Macromolecules.* 18: 2167–2173.

Howells, I. D. 1974. Drag due to the motion of a Newtonian fluid through a sparse random array of small fixed rigid objects. *J. Fluid Mech.* 64:449–475.

Hsu, T. P., and C. Cohen. 1984. Observation on the structure of a polyacrylamdie gel from electron micrographs. *Polymer.* 24:1419–1923.

Jackson, G. W., and D. F. James. 1986. The permeability of fibrous porous media. *Can. J. Chem. Eng.* 64:364–374.

Janas, V. F., F. Rodriguez, and C. Cohen. 1980. Aging and thermodynamics of polyacrylamide gels. *Macromolecules.* 13:977–983.

Johansson, G., G. Kopperschalager, and P. Albertsson. 1983. Affinity partitioning of phosphofructokinase from Baker's yeast using polymer-bound Cibacron blue F3G-A. *Eur. J. Biochem.* 43:589–594.

Johansson, L., and J. E. Löfroth. 1993. Diffusion and interaction in gels and solutions. 4. Hard sphere Brownian dynamics simulations. *J. Chem. Phys.* 98:7471–7478.

Johnson, E. M., D. A. Berk, R. K. Jain, and W. M. Deen. 1996a. Hindered diffusion in agarose gels: test of effective medium model. *Biophys. J.* 70:In press.

Johnson, E. M., D. A. Berk, R. K. Jain, and W. M. Deen. 1995b. Diffusion and partitioning of proteins in charged agarose gels. *Biophys. J.* 68: 1561–1568.

Khosrofian, J. M., and B. A. Garetz. 1983. Measurement of a Gaussian laser beam diameter through the direct inversion of knife-edge data. *Appl. Optics.* 22:3406–3410.

Kim, J. T., and J. L. Anderson. 1991. Diffusion and flow through polymer-lined micropores. *Ind. Eng. Chem. Res.* 29:1008–1016.

Laurent, T. C., I. Bjork, A. Pietruszkiewicz, and H. Persson. 1963. On the interaction between polysaccharides and other macromolecules. II. The transport of globular particles through hyaluronic acid solutions. *Biochim. Biophys. Acta.* 78:351–359.

Laurent, T. C., and A. Pietruszkiewicz. 1961. The effect of hyaluronic acid on the sedimentation rate of other substances. *Biochim. Biophys. Acta.* 49:258–264.

Lok, B. K., Y. L. Cheng, and C. R. Robertson. 1983. Total internal reflection fluorescence: a technique for examining interaction of macromolecules with solid surfaces. *J. Colloid Interface Sci.* 91:87–103.

Luby-Phelps, K., P. E. Castle, D. L. Taylor, and F. Lanni. 1987. Hindered diffusion of inert tracer particles in the cytoplasm of mouse 3T3 cells. *Proc. Natl. Acad. Sci. USA.* 84:4910–4913.

Morris, C. J. O. R., and P. Morris. 1971. Molecular-sieve chromatography and electrophoresis in polyacrylamide gels. *P. Biochem. J.* 124:517–528.

Munk, P., T. M. Aminabhavi, P. Williams, and D. E. Hoffman. 1980. Some solution properties of polyacrylamide. *Macromolecules.* 13:871–875.

Nagle, J. 1992. Long tail kinetics in biophysics? *Biophys. J.* 63:366–370.

Ogston, A. G. 1958. The spaces in a uniform random suspension of fibers. *Trans. Faraday Soc.* 54:1754–1757.

Park, I. H., J. C. S. Johnson, and D. A. Gabriel. 1990. Probe diffusion in polyacrylamide gels as observed by means of holographic relaxation methods: search for a universal equation. *Macromolecules.* 23: 1548–1553.

Patterson, G. D. 1987. Light scattering from gels. *Rubber Chem. Technol.* 62:498–513.

Phillips, R. J., W. M. Deen, and J. F. Brady. 1989. Hindered transport of spherical macromolecules in fibrous membranes and gels. *AIChE J.* 35:1761–1769.

Phillips, R. J., W. M. Deen, and J. F. Brady. 1990. Hindered transport in fibrous membranes and gels: effect of solute size and fiber configuration. *J. Colloid Interface Sci.* 139:363–373.

Rempp, P. J. 1957. Solutions of oxygenated straight-chain molecules. II. Intrinsic viscosities and coefficients of diffusion of translation of polyoxyethylene glycols. *J. Chim. Phys.* 54:432–453.

Righetti, P. G., C. Gelfi, and A. B. Bosisio. 1981. Polymerization kinetics of polyacrylamide gels. III. Effect of catalysts. *Electrophoresis.* 2:291–295.

Sellen, D. B. 1987. Laser light scattering study of polyacrylamide gels. *J. Polym. Sci.* 25:699–716.

Simon, J. R., A. Gough, E. Urbanik, F. Wang, F. Lanni, B. R. Ware, and D. L. Taylor. 1988. Analysis of rhodamine and fluorescein F-actin diffusion in vitro by fluorescence photobleaching recovery. *Biophys. J.* 54:801–815.

Tanaka, T. 1981. Gels. *Sci. Am.* 244:124–138.

Tilton, R. D. 1991. Surface diffusion and hydrophobic interactions in protein adsorption. Ph.D. thesis. Stanford University, Stanford, CA.

Tobita, H., and A. E. Hamielec. 1990. Crosslinking kinetics in polyacrylamide. *Polymer.* 31:1546–1552.

Tokita, M. 1993. Friction coefficient of polymer networks of gels and solvent. *In* Advances in Polymer Science 110. Responsive Gels: Volume Transitions II. K. Dusek, editor. Springer-Verlag, Berlin. 27–47.

Tong, J. 1995. Partitioning and diffusion of macromolecules in polyacrylamide gels. Ph.D. thesis. Carnegie Mellon University, Pittsburgh, PA.

Vasheghani-Farahani, E., D. G. Cooper, J. H. Vera, and M. E. Weber. 1992. Concentration of large biomolecules with hydrogels. *Chem. Eng. Sci.* 47:31–40.

Wagner, M. L., and H. A. Scheraga. 1956. Guoy diffusion studies of bovine serum albumin. *J. Phys. Chem.* 10:1066–1076.